Impact of Clustering in Statistical Indoor Propagation Models on Link Capacity

Kuo-Hui Li, Mary Ann Ingram, *Member, IEEE*, and Anh Van Nguyen, *Student Member, IEEE*

***Abstract*—Explicit clustering in a statistical indoor propagation model is found to have significant effects on the capacity of an array-to-array link or matrix channel. Effects of antenna spacing, Poisson homogeneity, block size, and transmit power allocation strategies are also considered.**

***Index Terms*—Array-to-array link, cluster, indoor wireless propagation models, MIMO.**

I. Introduction

Because of increased interest in smart antennas for wireless communications, there has been increased interest in statistical models that distinguish propagation paths in angle and delay. Several of these models explicitly cluster or bundle the rays in angle and delay, because clusters have been observed in measured data [1], [2].

In this paper, we consider the effects of explicit statistical clustering on the capacity of an array-to-array link. We find that the water-filling (WF) capacity [3] varies significantly (more than 4 b/s/Hz for SNRs 12 dB or higher) as a function of antenna spacing while there is no such variation for the unclustered model with the same total average path gain. Moreover, we find that clustering lowers the link capacity. We also consider the effect of modulating the average arrival rate in delay of the clusters, while maintaining the same average (over scenarios) power-delay profile (PDP).

II. Channel Modeling Backgroud

The models we use in our comparisons are based on the following three existing spatio-temporal models. The geometrically based single-bounce elliptical model has been proposed for mobile communications [4], [5]. In this model, the maximum delay of interest defines an ellipse, as shown in Fig. 1(a). The transmitter (TX) and the receiver (RX) are at the respective foci of the ellipse. A fixed number of point scatterers are distributed uniformly within this ellipse. The paths associated with these objects are assigned independent Rayleigh amplitudes with mean powers that obey an exponential decay.

Saleh and Valenzuela [1] were apparently the first to propose clustering for indoor propagation. Their model distinguished paths in time delay only. They modeled cluster arrival times using a homogeneous (i.e., constant average rate of arrival) Poisson process and modeled ray arrivals within a cluster with another homogeneous, but higher rate, Poisson process. They assigned Rayleigh amplitudes to each ray such that the Rayleigh average power obeys a product of two exponential decays, one for the clusters and one within each cluster. Based on a set of measured data, Spencer *et al.* [2] extended the Saleh–Valenzuela model to include angle-of-arrival (AOA) by assigning each cluster a "mean AOA" that is uniformly distributed across 360° and assigning ray AOAs within a cluster with independent Laplacian deviations from the mean AOA, with standard deviations of 25.5° or 21.5°.

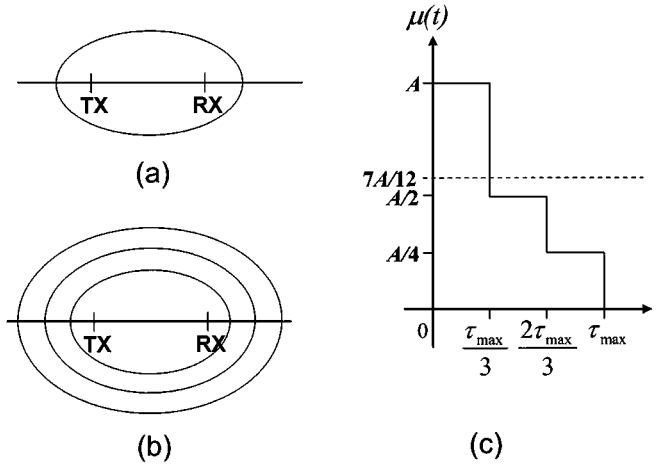

Fig. 1. (a) The unclustered model. (b) A three-subregion clustered model. (c) The cluster arrival rate of the nonhomogenous Poisson clustered model (NHPCM).

Lu *et al.* [6] proposed a nonhomogeneous clustered model based on elliptical subregions as shown in Fig. 1(b). The numbers of clusters in each subregion are independent Poisson random variables with different means for each subregion. The clusters are distributed uniformly within each elliptical subregion. The number of rays in each cluster are independently Poisson distributed. The AOAs are independent Gaussian deviations from the cluster center and the delays have independent exponential interarrivals. The ray amplitudes are assigned according to an exponential path loss law with lognormal shadowing.

III. Proposed Models

Our objective is to focus on the model features of clustering and of the homogeneity of cluster arrivals. We want the models to otherwise be as alike as possible. Also, we assume that exponential path loss dictates that the average of measured PDPs, if averaged over an increasing number of different indoor environments, would tend toward a limiting profile. Since each trial of a statistical model represents a different indoor environment, we ensure that our models produce nearly identical *average* PDPs.

Paper approved by F. Santucci, the Editor for Wireless System Performance of the IEEE Communications Society. Manuscript received July 15, 2000; revised December 15, 2000, and August 3, 2001. This work was supported by the Yamacraw Research Center of the State of Georgia. This paper was presented in part at the AP2000, Davos, Switzerland, April 9–14, 2000.

K.-H. Li was with the School of Electrical and Computer Engineering, Georgia Institute of Technology, Atlanta, GA 30332-0250 USA.

M. A. Ingram and A. Van Nguyen are with the School of Electrical and Computer Engineering, Georgia Institute of Technology, Atlanta, GA 30332-0250 USA (e-mail: mai@ece.gatech.edu).

Publisher Item Identifier S 0090-6778(02)03518-3.

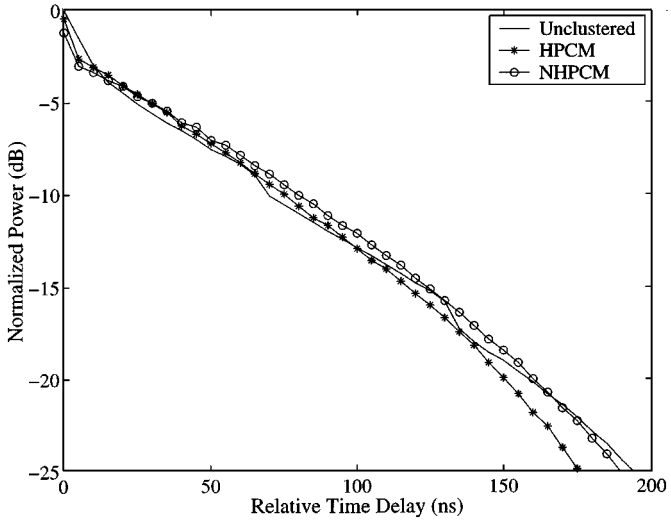

Fig. 2. The power delay of the unclustered and clustered models."0" on the horizontal axis corresponds to the delay of the shortest ray in each trial.

Furthermore, since power strongly impacts capacity, we scale all paths in a model to ensure that the average power is equal among the models.

We consider one unclustered and two clustered subregion models with the excess delay interval of [0, $\tau_{\max}$]. Each model consists of three subregions, corresponding to a uniform partition of the excess delay interval. One clustered model represents the nonhomogeneous case and the average rate of clusters is the solid-line stair-step function shown in Fig. 1(c). This model is designated as the nonhomogeneous Poisson clustered model (NHPCM). The other clustered model assumes the average rate of clusters is constant at $7A/12$, shown as the dashed line in Fig. 1(c) and is designated as homogeneous Poisson clustered model (HPCM). Once the number of clusters per subregion is determined for the respective models, the cluster locations are assigned as in the Lu *et al.* model [6] and the ray complex amplitudes, angles and delays are assigned as in the Spencer *et al.* model consistent with the Clyde Building [2]. The average number of rays in each subregion in the unclustered model is 40, which is the product of the average number of clusters in each subregion ($= 1$) times the average number of rays within a cluster ($= 40$) for the HPCM model. The average of the total number of rays is 120 for the HPCM and unclustered models. To shorten simulation time, all rays with energy less than 25 dB down from the strongest ray are eliminated. The averaged PDPs for these three models, averaged over 10 000 trials, are shown to be very close in Fig. 2. In these plots, "0" on the horizontal axis corresponds to the delay of the shortest ray in each trial.

Some other model and simulation parameters, common among the three models, are as follows. The pulse-shaping filter is the raised cosine filter, shared equivalently by the TX and RX, with a roll-off factor of 0.35 and a symbol period of $T = 10$ ns, which is smaller than the channel rms delay spread [8]. The pulse-shaping filter response is sampled over 10 symbol periods. Receiver sampling is synchronized to the peak of the line-of-sight pulse with a $T/2$ sampling rate. For the TX, perfect CSI is assumed for the WF scheme. Ten thousand trials are generated to compute the 1% outage rate capacity (b/s/Hz). The mean received SNR is defined as the average power for one transmit antenna in one symbol period times the SISO channel gain divided by the average noise power in one receive antenna.

IV. Capacities of Different Models

The WF capacity result of [7, eq. (5)] is used to compute the capacity of the wide-band multiple-antenna system. Two antenna configurations are considered: two transmit antennas with two receive antennas (2×2) and four transmit antennas with four receive antennas (4×4). We assume the RX has perfect channel-state information (CSI).

For the sake of computational convenience, the number of data symbols per block, N, is chosen to equal the number of antenna elements used at the TX. While a complete study of the effects of finite block length is beyond the scope of this paper, we considered a simple two-path space–time channel to show that changes in the block size would not affect the conclusions of this paper. We note that [7, Theorem 2] shows that in the limit as $N \to \infty$, the channel capacity becomes an integral over frequency, where for each frequency, the integrand is the capacity of the flat-fading array-to-array channel for that frequency. If the fractional bandwidth of the signal is small (as assumed in [7]), then the spatial properties of the channel, as indicated by the variation in the singular values of the flat-fading channel matrix, will be similar for all frequencies in the signal bandwidth. In this case, the effects of the spatial part of the channel will not be averaged out by the integration. In our study, we observed that the capacity for a given 2×2 or 4×4 channel smoothly decreased and approximately reached its limiting value for values of N less than 100. The total variation in the capacity of channels with large angle separation (corresponding to small disparities in the spatial-only channel singular values) was less than 0.5 b/s/Hz and for channels with small angle separation (large disparity in spatial-only singular values), the total variation was up to 3 b/s/Hz. Large disparity in singular values corresponds to lower capacity [10]. Therefore, the *difference* in capacities between channels with large and small angle separations should generally grow with N and approach limiting values. It follows that the differences that will be described in the next paragraph would be somewhat larger for larger block sizes, further emphasizing the conclusion of the paper.

The WF capacity versus the mean received SNR (dB) for the three models and for 2×2 and 4×4 systems are shown in Figs. 3 and 4, respectively. Let λ denote the wavelength. Antenna spacings of 0.5λ and 10λ are used. We observe that the capacity of the unclustered model is larger than that of the clustered models. For the clustered models, increasing antenna spacing from 0.5λ to 10λ increases the capacities by 2 and 4 b/s/Hz for the 2×2 and 4×4 systems, respectively, at 12 dB SNR or more. This happens because the rms angular spread of each cluster is narrow compared to the rms angular spread of the unclustered model and there are not many clusters (usually $\sim$ 2–3), resulting in correlated fading for 0.5λ spacing. Hence, increasing antenna spacing reduces the disparity of the singular values of the channel matrix. In constrast, the unclustered model is insensitive to the antenna spacing because of wider angular spreads. In spite of the correlated fading induced

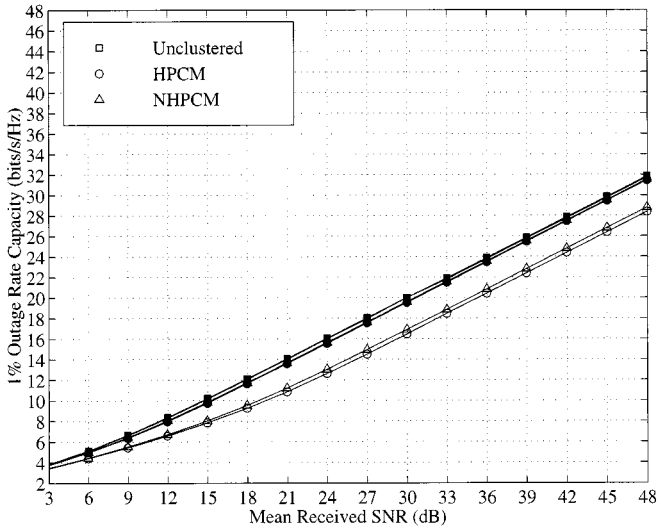

Fig. 3. The 1% outage rate capacity (b/s/Hz) as a function of the mean received SNR (dB) for the unclustered and clustered models with 0.5λ (open symbols) and 10λ (closed symbols) antenna spacing using the water-filling scheme in the 2×2 system.

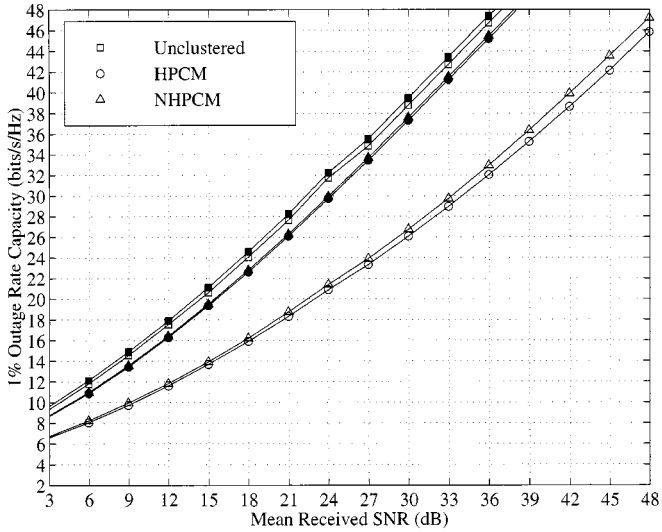

Fig. 4. The 1% outage rate capacity (b/s/Hz) as a function of the mean received SNR (dB) for the unclustered and clustered models with 0.5λ (open symbols) and 10λ (closed symbols) antenna spacing using the water-filling scheme in the 4×4 system.

by the clustering, the slopes of all of the 2×2 curves approach 2 b/s/Hz/3 dB and all of the 4×4 curves approach 4 b/s/Hz/3 dB at high SNR, as predicted by [7]. The capacities for the clustered models are lower than for the unclustered model because the clustered models need higher SNRs to reach their maximum slopes. We note that the capacity of the 4×4 unclustered model in Fig. 4 is somewhat higher than that of the 4×4 10-path channel considered in [7] mainly because of the difference in block sizes (4 versus 64, respectively).

Similar results can be found in [9]; however, in that paper, the capacity of unclustered model was not the highest compared to the other models as it is here. The difference can be attributed to the fact that in [9] the scatterers of the unclustered model were uniformly distributed in space over the entire ellipse defined by $[0, 2.7\tau_{\max}]$, even though the sum of path gains was conserved. The unclustered model in this paper yields a PDP more like the clustered models and therefore offers a more meaningful comparison.

Though not shown in this paper (see [8] for details), we find that the differences between the capacities of WF and equal-transmit-power (ETP) schemes are small for the 2×2 system, all less than 0.5 b/s/Hz. In the 4×4 case, there is is a difference of about 1.5 b/s/Hz for SNR from 0 dB to 15 dB for small antenna spacing but the differences are less for large spacing. This follows from the fact that clustering induces correlated fading over closely spaced antennas and correlated fading is known to produce a disparity between WF and ETP strategies [10]. We also find that both WF and ETP capacities reach their highest values for spacings exceeding 5λ.

V. Conclusion

The conclusions of this work are: 1) clustering makes both the water-filling and the equal-transmit power capacities sensitive to antenna spacing; 2) unclustered models overestimate the capacity if the paths of propagation are indeed clustered; and 3) there are no significant capacity differences between the homogeneous and nonhomogeneous clustered models when the average power-delay profile is conserved.

Acknowledgment

The authors would like to thank K. Tokuda and J.-S. Jiang for their assistance.

References

[1] A. A. Saleh and R. A. Valenzuela, "A statistical model for indoor multipath propagation," *IEEE J. Select. Areas Commun.*, vol. SAC-5, pp. 128–137, Feb. 1987.

[2] Q. Spencer, M. Rice, B. Jeffs, and M. Jensen, "A statistical model for angle of arrival in indoor multipath propagation," in *Proc. 1997 IEEE Veh. Technol. Conf.*, vol. 3, Phoenix, AZ, May 4–7, 1997, pp. 1415–1419.

[3] T. M. Cover and J. A. Thomas, *Elements of Information Theory*. New York: Wiley, 1991.

[4] J. C. Liberti and T. S. Rappaport, "A geometrically based model for line-of-sight multipath radio channels," in *Proc. 1996 IEEE Veh. Technol. Conf.*, vol. 2, Atlanta, GA, April 1, 1996, pp. 844–848.

[5] W. R. Braun and U. Dersch, "A physical mobile radio channel model," *IEEE Trans. Veh. Technol.*, vol. 40, pp. 472–482, May 1991.

[6] M. Lu, T. Lo, and J. Litva, "A physical spatio-temporal model of multipath propagation channels," in *Proc. 1997 IEEE Vehic. Tech. Conf.*, vol. 2, Phoenix, AZ, May 4–7, 1997, pp. 810–814.

[7] G. G. Raleigh and J. M. Cioffi, "Spatio-temporal coding for wireless communication," *IEEE Trans. Commun.*, vol. 46, pp. 357–366, Mar. 1998.

[8] K.-H. Li, "RF Beamformers for High-Speed Wireless Communications," Ph.D., Georgia Inst. Technology, Atlanta, Georgia, 2000.

[9] K.-H. Li and M. A. Ingram, "Impact of clustering in statistical indoor propagation models on link capacity," in *Proc. AP2000 Millennium Conf. Antennas Propag.*, Davos, Switzerland, April 9–14, 2000.

[10] D.-S. Shiu, "Wireless communications using dual antenna array," Ph.D. dissertation, Univ. California, Berkeley, 1999.